Cooperative Therapeutic Action of Retinoic Acid Receptor and Retinoid X Receptor Agonists in a Mouse Model of Alzheimer's Disease

Kohichi Kawahara[a,b,1,*], Michita Suenobu[a,b,1], Hideyuki Ohtsuka[a,b], Akihiko Kuniyasu[a,b],
Yukihiko Sugimoto[b], Madoka Nakagomi[c], Hiroshi Fukasawa[c], Koichi Shudo[c] and Hitoshi Nakayama[a,*]
[a]*Department of Molecular Cell Function, Faculty of Life Sciences, Kumamoto University, Kumamoto, Japan*
[b]*Department of Pharmaceutical Biochemistry, Faculty of Life Sciences, Kumamoto University, Kumamoto, Japan*
[c]*Research Foundation ITSUU Laboratory, Setagaya-ku, Tokyo, Japan*

Handling Associate Editor: Shun Shimohama

Abstract. Alzheimer's disease (AD) is a neurodegenerative process involving amyloid-β (Aβ) peptide deposition, neuroinflammation, and progressive memory loss. Here, we evaluated whether oral administration of retinoic acid receptor (RAR)α,β agonist Am80 (tamibarotene) or specific retinoid X receptor (RXR) pan agonist HX630 or their combination could improve deficits in an AD model, 8.5-month-old amyloid-β protein precursor 23 (AβPP23) mice. Co-administration of Am80 (0.5 mg/kg) and HX630 (5 mg/kg) for 17 days significantly improved memory deficits (Morris water maze) in AβPP23 mice, whereas administration of either agent alone produced no effect. Only co-administration significantly reduced the level of insoluble Aβ peptide in the brain. These results thus indicate that effective memory improvement via reduction of insoluble Aβ peptide in 8.5-month-old AβPP23 mice requires co-activation of RARα,β and RXRs. RARα-positive microglia accumulated Aβ plaques in the AβPP23 mice. Rat primary microglia co-treated with Am80/HX630 showed increased degradation activity towards ^{125}I-labeled oligomeric Aβ_{1-42} peptide in an insulin-degrading enzyme (IDE)-dependent manner. The co-administration increased mRNA for IDE and membrane-associated IDE protein *in vivo*, suggesting that IDE contributes to Aβ clearance in Am80/HX630-treated AβPP23 mice. Am80/HX630 also increased IL-4Rα expression in microglial MG5 cells. The improvement in memory of Am80/HX630-treated AβPP23 mice was correlated with the levels and signaling of hippocampal interleukin-4 (IL-4). Therefore, Am80/HX630 may promote differentiation of IL-4-responsive M2-like microglia and increase their activity for clearance of oligomeric Aβ peptides by restoring impaired IL-4 signaling in AβPP23 mice. Combination treatment with RAR and RXR agonists may be an effective approach for AD therapy.

Keywords: Alzheimer's disease, Am80, amyloid-β peptides, HX630, interleukin-4, memory improvement

INTRODUCTION

Alzheimer's disease (AD) is a serious neurodegenerative disorder with no effective treatment. Its onset and progression correlate with neuroinflammatory processes [1], and inflammatory microglia are associated with AD-like pathology in a transgenic mouse model [2, 3].

---

[1]These authors contributed equally to this work.

*Correspondence to: Drs. Hitoshi Nakayama and Kohichi Kawahara, Department of Molecular Cell Function, Faculty of Life Sciences, Kumamoto University, Kumamoto 862-0973, Japan. Tel.: +81 96 371 4358; Fax: +81 96 372 7182; E-mails: jin@gpo.kumamoto-u.ac.jp; kkawa@gpo.kumamoto-u.ac.jp (Kohichi Kawahara).

Retinoids are analogues of vitamin A-derived all-*trans* retinoic acid (ATRA), and are specific modulators of many cellular functions, including immunity [4]. Retinoic acid (RA) exerts its biological actions by binding to its cognate nuclear receptors, retinoic acid receptors (RARs), which heterodimerize with retinoid X receptors (RXRs) to regulate transcription of target genes. Each of them has three subtypes: RARα,β,γ and RXRα,β,γ.

Vitamin A deprivation results in Aβ accumulation in rats [5]. RA increases gene transcription of a disintegrin and metalloprotease, family 10 (ADAM10) [6–8] and increases its α-secretase activity, which cleaves a specific site of amyloid-β protein precursor (AβPP). This cleavage inhibits Aβ generation and leads to release of the soluble neuroprotective protein sAβPPα [9–11]. Clinical evidence has indicated that late-onset AD brains have a defect in retinoid transport function [12]. Therefore, RA or synthetic retinoids may be candidates for treatment of AD [5, 13–17]. We previously demonstrated that oral administration of Am80 (0.5 mg/kg/d, for 14 weeks) reduced levels of Tris-buffered saline (TBS)-insoluble $A\beta_{42}$ in brains of 5-month-old AβPP23 mice, an AD model [15]. However, that study did not detect behavioral benefits of this treatment. Recently, Cramer et al. [16] reported that the RXR-selective agonist bexarotene enhanced apolipoprotein E-dependent Aβ clearance from the brain and improved behavioral deficits in AβPP/PS1 mice. However, there are conflicting data regarding the therapeutic effect of bexarotene on AβPP mice [18–22]. Furthermore, it remains unclear whether co-activation of RARs with RXRs is required to improve AD pathology and memory deficits.

Retinoids modify T helper (Th) types 1 and 2 cells and regulatory T-cell-associated immune responses in rodents and humans [23]. They also suppress Th1 development and enhance development of naïve CD4 T cells to interleukin (IL)-4-producing Th2 cells [24]. IL-4 plays an essential role in higher functions, such as memory and learning, of normal brain [25]. For example, IL-4-deficient mice show cognitive impairment in spatial learning tasks [26]. However, it remains unclear whether retinoids affect AD-associated neuroinflammatory processes *in vivo*.

In this study, we investigated whether a combination of RARα,β agonist Am80 [27, 28] and RXR pan agonist HX630 [29, 30] would produce any memory improvement in AβPP23 mice. We also determined the brain levels of TBS-soluble and TBS-insoluble Aβ and several molecules related to Aβ metabolism (including degradation and phagocytotic clearance of Aβ *in vivo*

and *in vitro*) before and after the retinoid treatments. We also examined the effects of Am80 and HX630 on neuroinflammatory processes in AβPP23 mice.

MATERIALS AND METHODS

Compounds

Tamibarotene (also known as Am80) and HX630 were prepared as previously described [31, 32]. GW9662 was obtained from Cayman Chemical (Ann Arbor, MI, USA). These compounds were dissolved in DMSO for *in vitro* study (stock solution: 10 mM).

Animals

Hemizygous AβPP23 mice, which overexpress human-type AβPP carrying the double mutation K670 N/M671 L, were produced and bred as previously described [33]. Only male mice were analyzed. Wistar rats were obtained from Kyudo Co., Ltd. (Kumamoto, Japan). Animals were housed in standard mouse cages under standard laboratory conditions: food and water available *ad libitum*, constant room temperature and humidity, and a 12 h light/12 h dark cycle (light on from 08 : 00 to 20 : 00). These animal experiments were conducted according to the guidelines of the Ministry of Education, Culture, Sports, Science, and Technology of Japan, and were approved by the Institutional Animal Care and Use Committee of Kumamoto University (#B25-133).

Cell culture

Primary microglia (type 1) were harvested from primary mixed glial cell cultures prepared from neonatal Wistar rat pups, as previously reported [34]. Mouse microglial cell line MG5 and mouse glial cell line A1 were maintained as previously described [35]. Mouse neuroblastoma cell line N1E-115 and Neuro 2a (American Type Culture Collection, Manassas, VA, USA) were maintained in Dulbecco's modified Eagle's medium (DMEM) supplemented with 10% fetal bovine serum (FBS), 20 U/ml penicillin (Invitrogen, Gaithersburg, MD, USA), and 20 μg/ml streptomycin (Invitrogen). Primary rat microglia were treated with Am80 (5 μM) and/or HX630 (5 μM) in the presence and absence of GW9662 (10 μM) for 48 h in Eagle's MEM supplemented with 10% FBS and 0.2% glucose. MG5 cells and A1 cells were treated with Am80 (5 μM) and/or HX630 (5 μM) for 48 h in DMEM containing 10% FBS.

N1E-115 cells were treated with Am80 (5 μM) and/or HX630 (5 μM) for 5 days in DMEM containing 2% FBS.

Since the effective concentration of Am80 *in vivo* has not been determined, we considered that a relatively high concentration of Am80 should be used in the *in vitro* study in order to ensure adequate stimulation. When we investigated RARE-luciferase activity in Neuro2a cells, Am80 in the concentration range of 0.2–5 μM hardly altered the RARE activity (Supplementary Figure 1). Moreover, the combination of HX630 (5 μM) with Am80 in the range of 0.2–5 μM also had little effect. Therefore, the concentrations of Am80 and HX630 were both set at 5 μM for the *in vitro* study.

Cell assays

^{125}I-Labeled oligomeric Aβ$_{1-42}$ (o-Aβ$_{1-42}$) was prepared as described [34]. Cells were cultured in 24-well plates for 48 h in Eagle's MEM supplemented with 10% FBS in the presence or absence of Am80 (5 μM) and HX630 (5 μM). After the 48-h treatment, the cells were washed twice with labeling medium (DMEM containing 3% BSA) and then incubated with ^{125}I-labeled o-Aβ$_{1-42}$ for 6 h at 37°C. Following the 6-h incubation, medium was removed from each well, and soluble radioactivity in TCA (degraded and extracellularly released peptide fragments) was determined as an index of Aβ degradation in the medium as described previously [34]. The Aβ degradation activity may thus include both receptor-mediated phagocytic activity and extracellular protease-mediated degradation. Cells were washed three times with PBS, then lysed with 0.4 ml of 0.1 M NaOH for 30 min at 37°C, and cell-associated (including cell-incorporated) radioactivity and cell proteins were determined with an autogamma counter and the BCA Protein Assay Reagent (Pierce), respectively. We could not determine the activity of IDE-dependent degradation in this medium, because the incubation medium was replaced with labeling medium prior to incubation with ^{125}I-o-Aβ.

Drug administration

AβPP23 mice begin forming amyloid deposits when they are 6 months old, but memory deficits in the MWM test appear quite early (before 3 months of age) [36]. Here, we used 8.5-month-old male AβPP23 mice and their wild-type (WT) littermates (C57BL/6J). We used stratified random sampling to divide mice (four to

six per cage) into four groups to equalize the mean body weight of the study groups: mice given 0.5 mg/kg/d Am80, those given 5 mg/kg/d HX630, those given the mixture of 0.5 mg/kg/d Am80 and 5 mg/kg/d HX630, and those given the vehicle. Am80 and HX630 were suspended in 0.5% (w/v) carboxymethylcellulose solution and were orally administered to mice at 0.5 mg/kg (Am80) or 5 mg/kg (HX630) for 17 consecutive days (once daily at 18 : 00). Control animals received the same volume of 0.5% (w/v) carboxymethylcellulose solution orally, without the other compounds. We set the 0.5 mg/kg/d dose for Am80 on the basis that this had been found effective in other *in vivo* studies, such as those by Kawahara et al. [15] and Ishido and Shudo [37]. Higher doses of Am80 (3 mg/kg/d and 6 mg/kg/d) were also orally administered to mice for 17 consecutive days. Animals were weighed once a week. Mice were subjected to behavioral testing on days 15–18 of the first oral administration of the compounds (at 19 : 00–23 : 00). On days 15–17 (not day 18), animals received the compounds at 24 : 00, after behavioral testing. On the last day of behavioral testing (day 18), animals received no compounds and tissues were sampled.

Morris water maze (MWM) test

The MWM test was performed as described previously [15, 38]. For this test, administered during the 12 h dark period, a circular, 150-cm-diameter pool (40 cm high) was filled with water maintained at 23.0 ± 1°C. A 12-cm-diameter round platform was placed in one quadrant and was kept 1 cm below the water surface. During acquisition training, mice completed three to five trials daily for 4 consecutive days: day 1 : 3 trials, day 2 : 3 trials, day 3 : 5 trials, and day 4 : 4 trials. The trials began at three different positions in semirandom order, and intertrial intervals were 20 min. A mouse that could not find the platform in 120 s was carefully guided to the platform and was allowed to stay there for 20 s. A probe trial followed the acquisition phase: the platform was removed from the maze, and mice were permitted to swim freely for 100 s. During both acquisition and probe trials, the routes of the mice were recorded by means of a computerized video tracking system (CompACT VAS; Muromachi Kikai Co. Ltd., Tokyo, Japan). Training trials measured the time it took for a mouse to find the escape platform. Probe trials determined the percent time spent in each quadrant of the maze. The number of times that a mouse crossed over the training annulus (diameter of 22 cm), which was 3.1 times

the size of the target platform, was also used to analyze performance in the probe trial. In this study, the probe trial was administered at 2 h after the last training trial. Spatial memory retention of the platform position is considered to reflect short-term memory [39].

Animal tissue sampling

After the behavior analysis (at 2 h after the probe trial), mice were anesthetized with an injection of Somnopentil (50 mg/kg, given intraperitoneally; Kyoritsu Seiyaku, Tokyo, Japan), after which they were perfused transcardially with 30 ml of PBS. Brains were rapidly removed and divided into hemispheres. One hemisphere was snap-frozen in liquid nitrogen for protein analysis. The other hemisphere was snap-frozen in liquid nitrogen for total RNA assay. In some experiments, a hemisphere was divided under a stereomicroscope into four sections: cerebral cortex, hippocampus, cerebellum, and other regions, each of which was snap-frozen in liquid nitrogen and stored at $-80°C$ until use. The number (n) of mice used for experiments is shown in each figure.

Immunoblot analysis

Rat primary microglia and mouse microglial MG5 cells (5×10^6 cells per 100-mm dish) were homogenized in RIPA buffer [10 mM Hepes-NaOH (pH 7.4) containing 150 mM NaCl, 1 mM EDTA, 1% Triton X-100, 0.5% sodium deoxycholate, 0.1% SDS, 1 mM PMSF, 1 mg/ml leupeptin, 1 mg/ml pepstatin A, and 10 mg/ml soybean trypsin inhibitor]. After centrifugation of samples, supernatants were separated by SDS-PAGE and proteins were electrotransferred to nitrocellulose membranes. The cerebral hemispheres and hippocampus were homogenized in 3 volumes (w/v) and 10 volumes (w/v), respectively, of 50 mM Tris-HCl buffer (pH 7.6) containing 150 mM NaCl, 1 mM PMSF, 1 mg/ml leupeptin, 1 mg/ml pepstatin A, and 10 mg/ml soybean trypsin inhibitor. Triton X-100-solubilized membrane fractions of the cerebral hemispheres were prepared as described previously [40]. Aliquots of homogenates and membrane fractions were saved for determination of protein, and, after addition of 25 mM DTT, samples were incubated at 60°C for 10 min. The samples (40 μg homogenate or 5.0 μg membrane fraction) were then subjected to SDS-PAGE, and proteins were electrotransferred to nitrocellulose membranes. These membranes were incubated with Tris-buffered saline (TBS) (pH 7.4)

containing 2% dehydrated skimmed milk to block nonspecific protein binding. Membranes were then incubated with antibodies to CD36 (BAF2519, 1 : 500 dilution; R&D Systems), NEP (H-321, 1 : 100 dilution; Santa Cruz Biotechnology, Santa Cruz, CA, USA), IDE (PC730, 1 : 1000 dilution; Calbiochem, Darmstadt, Germany; 9B12, 1 : 1000 dilution; Abcam, Cambridge, UK), IL-4 receptor α chain (IL-4Rα) (S-20, 1 : 200 dilution; Santa Cruz Biotechnology), $Aβ_{1-17}$ (6E10, 1 : 500 dilution; Chemicon International, Temecula, CA, USA), scavenger receptor class AI/AII (SRA) (SRA-E5, 1 : 1000 dilution; a gift from Prof. M. Takeya at Kumamoto University, Kumamoto, Japan), or β-actin (AC15, 1 : 5000 dilution; Sigma), followed by secondary antibodies: horseradish peroxidase-linked antibodies against rabbit, goat, or mouse Ig (each diluted 1 : 1000). Bound horseradish peroxidase-labeled antibodies were then detected via chemiluminescence (an ECL kit; Pierce, Rockford, IL, USA). Protein concentrations were determined with the BCA Protein Assay Reagent (Pierce) and Bradford Protein Assay Reagent (Pierce).

Immunohistochemistry

Mice were anesthetized with pentobarbital, and 4% PFA in PBS was perfused through the left cardiac ventricle. Brains were removed and embedded in paraffin, before being cut into 4 μm thick sections, which were then deparaffinized and incubated with 0.01% (w/v) 1-fluoro-2,5-bis(3-carboxy-4-hydroxystyryl)benzene (FSB, a reagent for amyloid staining; Dojindo, Kumamoto, Japan) for 30 min. After washing with 50% ethanol, the sections were autoclaved (at 120°C) in 10 mM citrate buffer (pH = 6.0) for 5 min, and washed in PBS. For Aβ staining (6E10), sections were immersed in 70% formic acid for 10 min. The sections were then incubated with primary antibodies to RARα (rabbit IgG, C-20, 1 : 100 dilution; Santa Cruz Biotechnology), RARβ (rabbit IgG, C-19, 1 : 100 dilution; Santa Cruz Biotechnology), $Aβ_{1-17}$ (mouse IgG, 6E10, 1 : 500 dilution; Chemicon International, Temecula, CA, USA), Iba1 (rat serum, 1 : 500 dilution; generated against a synthetic peptide corresponding to a specific sequence of mouse Iba1: CNKEHKRPTGPPAKKAISELP (near the C-terminus)), or GFAP (chicken IgY, GTX85454, 1 : 200 dilution; GeneTex), followed by the corresponding Alexa Fluor 488- or 594-labeled secondary antibodies (1 : 300 dilution; Molecular Probes and Abcam). For immunohistochemistry with anti-Iba1 antibody, we used a tyramide signal amplification

system (Molecular Probes) according to the manufacturer's recommendations. Specimens were mounted with VECTASHIELD mounting medium (Vector) and were examined with a confocal laser-scanning microscope (FluoView; Olympus).

For immunohistochemical staining with IL-4Rα, the avidin-biotin peroxidase technique was used. Mice were anesthetized with pentobarbital, and 4% PFA in PBS was perfused through the left cardiac ventricle. Brains were removed and cryoprotected in sucrose. Frozen sections (10-μm thick) were cut with a cryostat and thaw-mounted on gelatin-coated slides. The coronal sections were immersed in 10 mM citrate buffer (pH = 6.0) and were autoclaved (at 80°C) for 5 min. Endogenous peroxidase was blocked by treatment with 1% H_2O_2 in methanol for 15 min, followed by overnight incubation at 4°C with rabbit anti-IL-4Rα antibody (S-20, 1 : 100 dilution; Santa Cruz Biotechnology). Rabbit IgG from non-immune serum was used as a negative control. Excess antibody was washed out with PBS, and the sections were incubated for 1 h with the corresponding biotinylated secondary antibody (1 : 200 dilution, Chemicon International). The sections were then incubated for 30 min at room temperature with avidin-peroxidase complex (Vector). Peroxidase was visualized by incubation with diaminobenzidine solution with nickel enhancement.

ELISA

The TBS-soluble (TBS-extractable) fraction and the TBS-insoluble (but guanidine HCl-extractable) fraction from the cerebral hemispheres or hippocampus were prepared as described previously [15, 41]. The amounts of $A\beta_{40}$ and $A\beta_{42}$ in each fraction were determined by using sandwich ELISAs (294-64701 and 290-62601 (Wako), respectively), according to the manufacturer's instructions. The amounts of tumor necrosis factor-α (TNF-α) and IL-4 in the TBS-soluble fractions of cerebral cortex and hippocampus were analyzed by means of sandwich ELISAs KMC3012 (Invitrogen) and ELM-IL-4-001 (RayBiotech, Inc., Norcross, GA, USA), respectively, according to the manufacturer's instructions. Protein concentrations were determined with the Bradford Protein Assay Reagent (Thermo Fisher Scientific Inc., Rockford, IL, USA), with BSA as the standard.

RT-PCR Analysis

Total RNA from the cerebral hemispheres, hippocampus, or MG5 cells was prepared by guanidinium thiocyanate-phenol-chloroform extraction [42]. Then, 1.0 μg of total RNA was converted to cDNA with SuperScript III Reverse Transcriptase (Invitrogen) and nucleotide random primer (Invitrogen). Quantitative real-time PCRs were carried out by using the LightCycler 1.5 system (Roche, Mannheim, Germany) with the FastStart DNA Master SYBR Green I LightCycler kit (Roche). The primers used were as follows: for *Ide*: sense primer, 5′-CGGCCAT CCAGAGAATAGAA-3′ and antisense primer, 5′-TTT GGAGGGTCTGACAGTGA-3′; for *Il4rα*: sense primer, 5′-CCTCACACTCCACACCAATG-3′ and antisense primer, 5′-CCTGGGTTCCTTGTAGGT CA-3′; for *Tnf receptor (Tnfr)1*: sense primer, 5′-ACGGCTTCCCAGAATTACCT-3′ and antisense primer, 5′-TCAGCTTGGCAAGGAGAGAT-3′; for *Tnfr2*: sense primer, 5′-TACCAAGGGTGGCATCTC TC-3′ and antisense primer, 5′-AGGGCTTCTT TTTCCTCTGC-3′; for *RARα (rarα)*: sense primer, 5′-TTCTTTCCCCCTATGCTGGGT-3′ and antisense primer, 5′-GGGAGGGCTGGGTACTATCTC-3′; for *RARβ (rarβ)*: sense primer, 5′-CTGCTCAATCCAT CGAGACAC-3′ and antisense primer, 5′-CTTG TCCTGGCAAACGAAGC-3′; for tissue-plasminogen activator (*tPA*): sense primer, 5′-ATGAGGCATC GTCTCCATTC-3′ and antisense primer, 5′-ACAGA TGCTGTGAGGTGCAG-3′; and for *β-actin*: sense primer, 5′-CTAAGGCCAACCGTGAAAAG-3′ and antisense primer, 5′-ACCAGAGGCATACAGGGA CA-3′. A standard curve for each gene was generated with serial dilutions of the respective PCR product. Expression was normalized against the expression of *β-actin*. PCR specificity was confirmed by means of sequencing, gel electrophoresis, and melting curve analysis.

For semi-quantitative RT-PCR analysis, PCRs were carried out with Quick Taq HS DyeMix (DTM-101; Toyobo Co. Ltd., Osaka, Japan). The primers used were as follows: for *Cd36*: sense primer, 5′-AGGTCCTTACACATACAGAGTTCG-3′ and antisense primer, 5′-GGACTTGCATGTAGGAAATGT GGA′; for *membrane metallo-endopeptidase (Mme)/ Nep*: sense primer, 5′-CAGCCTCAGCCGAAACTA-CA-3′ and antisense primer, 5′-TTTGTCTCAGCA-TCCATCCAA-3′; for *Ide*: sense primer, 5′-CGGCCA-TCCAGAGAATAGAA-3′ and antisense primer, 5′-TT TGGAGGGTCTGACAGTGA-3′; for β-actin: sense primer, 5′-CTAAGGCCAACCGTGAAAAG-3′ and antisense primer, 5′- ACCAGAGGCATACAGGGA CA-3′. The primer sets for *Cd36*, *Mme*, *Ide,* and β-actin were expected to give PCR products with sizes of 789, 255, 172, and 104 bp, respectively. Semi-quantitative

PCR consisted of an initial denaturation cycle at 94°C for 2 min, followed by 40 cycles for *Cd36*, 35 cycles for *Mme*, 30 cycles for *Ide*, and 26 cycles for *β-actin*. An additional cycle at 72°C for 7 min completed the amplification. Amplified PCR products were separated by 2% (except for *Cd36*, 1.5%) agarose gel electrophoresis and visualized by staining with ethidium bromide. Densitometric quantification was done with the Image Gauge software program (Fuji Photo Film Co., Tokyo, Japan). Expression was normalized against the expression of β-*actin*. PCR specificity was confirmed by means of sequencing and gel electrophoresis.

Transient transfection and reporter gene assay

MG5 cells (2×10^6 cells in 100 μl) were transfected by electroporation with 1.0 μg of pGL3-RARE-Luc (#13458; Addgene) or pGL3-Luc vector (Promega) and 0.25 μg of *Renilla* luciferase vector (phRL-TK) (Promega), using the Nucleofector transfection system (program #D-032; Amaxa) according to the manufacturer's protocol, taken up in the medium, and seeded in 48-well plates (1.25×10^5 cells/well). For some experiments, cells were transfected with 1.0 μg of pGL3-RARE-Luc or pGL3-Luc vector and 0.25 μg of phRL-TK in the presence of 0.25 μg each of pcDNA3.1-RAR (#16287; Addgene) and pcDNA3.1-RXR (#8882; Addgene). An empty pcDNA3.1 expression vector was used to maintain equal amounts of DNA for each transfection. Five hours after transfection, the cells were exposed to Am80 (5 μM) and/or HX630 (5 μM) in the medium for 24 h. Luciferase activities were determined in cell lysates. Firefly luciferase activity was normalized to that of *Renilla* luciferase for each well.

Neuro2a cells were seeded in 24-well plates (2×10^5 cells/well) and transfected with 0.2 μg of pGL3-RARE-Luc (#13458; Addgene) or pGL3-Luc vector (Promega) and 0.05 μg of *Renilla* luciferase vector (phRL-TK) (Promega), using Effectene reagent (Qiagen) according to the manufacturer's protocol. Five hours after transfection, cells were exposed to Am80 (5 μM) and/or HX630 (5 μM) in the medium for 24 h. Luciferase activities were determined in cell lysates. Firefly luciferase activity was normalized to that of *Renilla* luciferase for each well.

Statistical analysis

All data were expressed as means ± SEM. For statistical comparisons of the means between two groups, Student's *t*-test was applied after confirming the equal-ity of group variances. In factorial ANOVA, drug treatment (vehicle, Am80, HX630, or Am80/HX630) was used as a between-subject factor and the training regimen (days or trials) was used as a within-subject (repeated measures) factor. The Bonferroni multiple comparison test was used after two-way ANOVA. For comparisons of three or more groups, Dunnett's multiple comparison test was applied after one-way ANOVA. To determine whether a correlation between variables existed, a scatterplot and Pearson correlation analyses were employed. All statistical analyses were performed with GraphPad Prism (GraphPad Software). Significance was defined as *p* value <0.05.

RESULTS

Co-administration of Am80 with HX630 reversed deficits in spatial learning and memory in 8.5-month-old AβPP23 mice

We orally administered tamibarotene/Am80 (a selective RARα,β agonist with little or no binding affinity for RARγ and RXRs, 0.5 mg/kg), HX630 (a pan RXRs agonist, 5 mg/kg), or their combination to 8.5-month-old AβPP23 mice (an AD model) and their WT littermates for 17 days (Fig. 1A). During the experimental period, body weights of the mice in the different groups showed no significant difference (data not shown). Vehicle-treated AβPP23 mice showed considerably impaired acquisition of spatial learning (i.e., a longer escape latency) in the MWM test, compared with WT littermates (Fig. 1B; *p* < 0.001 by two-way ANOVA). However, co-administration of Am80 with HX630 to AβPP23 mice led to a significant improvement in this measure compared with vehicle-injected control AβPP23 mice (Fig. 1B; *p* < 0.001 by two-way ANOVA). In addition, a *post hoc* comparison indicated that significant improvement was detected only in the co-administration group, not in groups treated with either agonist alone (Fig. 1B; *p* < 0.01). In the *post hoc* comparison among groups, Am80/HX630 co-treatment showed a significant improvement compared with either HX630 treatment (at days 2–4) or Am80 treatment (at days 2 and 3, but not at day 4).

After the acquisition trials, mice underwent probe trials to evaluate retention of memory of the platform location (Fig. 1C). Vehicle-treated AβPP23 mice spent a significantly shorter time in the target quadrant (17.1 ± 3.6%) compared with vehicle-treated WT mice (33.0 ± 3.2%) (Fig. 1C; *p* < 0.01). However, Am80/HX630-treated AβPP23 mice spent a significantly longer time in the target quadrant (30.5 ± 6.1%)
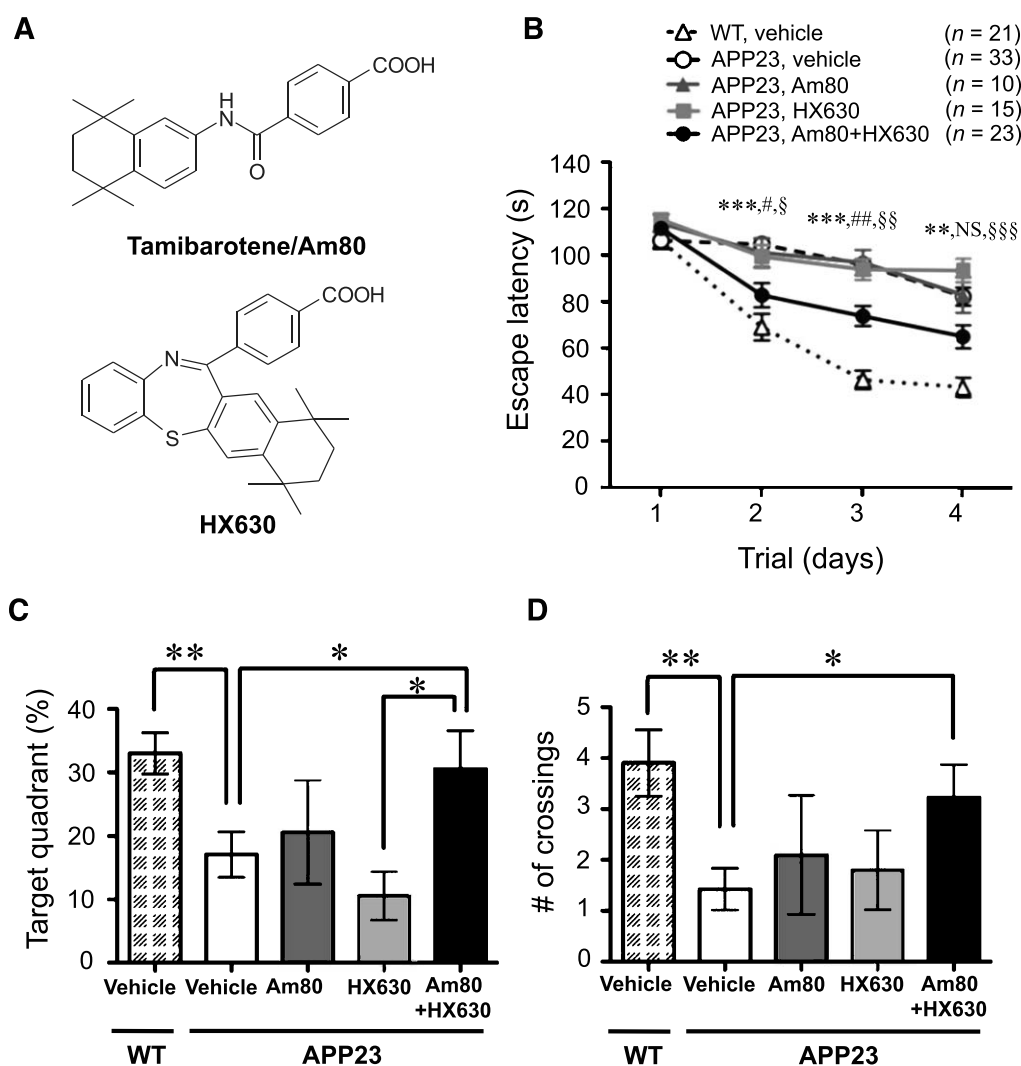
Fig. 1. Co-administration of Am80 with HX630 reversed deficits in spatial learning and memory in 8.5-month-old male AβPP23 mice. A) Chemical structure of synthetic retinoids, tamibarotene/Am80, and HX630. B-D) Am80 and/or HX630 were orally administered to mice at 0.5 mg/kg (Am80) or 5 mg/kg (HX630) for 17 consecutive days. Spatial learning and memory were evaluated by means of the MWM test from day 15 to day 18 of the first oral administration of the compounds. Error bars represent means ± SEM ($n = 21$ in vehicle-treated WT mice, $n = 33$ in vehicle-treated AβPP23 mice, $n = 10$ in Am80-treated AβPP23 mice, $n = 15$ in HX630-treated AβPP23 mice, $n = 23$ in Am80/HX630-treated AβPP23 mice). B) For 4 consecutive days, mice learned to swim to a hidden platform. Each point indicates the mean latency to find the escape platform in three to five trials per day ± SEM for each group. Statistical significance of differences was calculated by using two-way ANOVA followed by the *post hoc* Bonferroni multiple comparison test. Significant differences with ***$p < 0.001$ (at days 2 and 3) and **$p < 0.01$ (at day 4) were detected between Am80/HX630-treated AβPP23 mice and vehicle-treated ones. Differences between Am80/HX630-treated AβPP23 mice and Am80-treated ones were observed as #$p < 0.05$ (at day 2), ##$p < 0.01$ (at day 3), and not significant (NS, at day 4) Significant differences between Am80/HX630-treated AβPP23 mice and HX630-treated ones were detected as §$p < 0.05$ (at day 2), §§$p < 0.01$ (at day 3), and §§§$p < 0.001$ (at day 4). No significant difference was observed among the three groups: vehicle-treated, Am80-treated, and HX630-treated AβPP23 mice. C, D) Memory test in the MWM probe trial without the platform. The probe trial was administered at 2 h after the last training trial (i.e., at day 18 after the start of treatment). Measures included (C) the time (%) spent searching the target quadrant and (D) the number of crossings over the training annulus (3.1×the size of the target platform) during a probe trial (a 100-s session). **$p < 0.01$ and *$p < 0.05$ by Student's *t*-test. No significant difference was observed for Am80/HX630 co-treatment relative to the Am80 (C, D) and HX630 treatments (D).

than did vehicle-treated AβPP23 mice (Fig. 1C; $p < 0.05$). In addition, Am80/HX630-treated AβPP23 mice spent a significantly longer time in the tar-

get quadrant than did HX630-treated mice (Fig. 1C; $p < 0.05$). As expected, vehicle-treated AβPP23 mice had significantly fewer crossings over the training
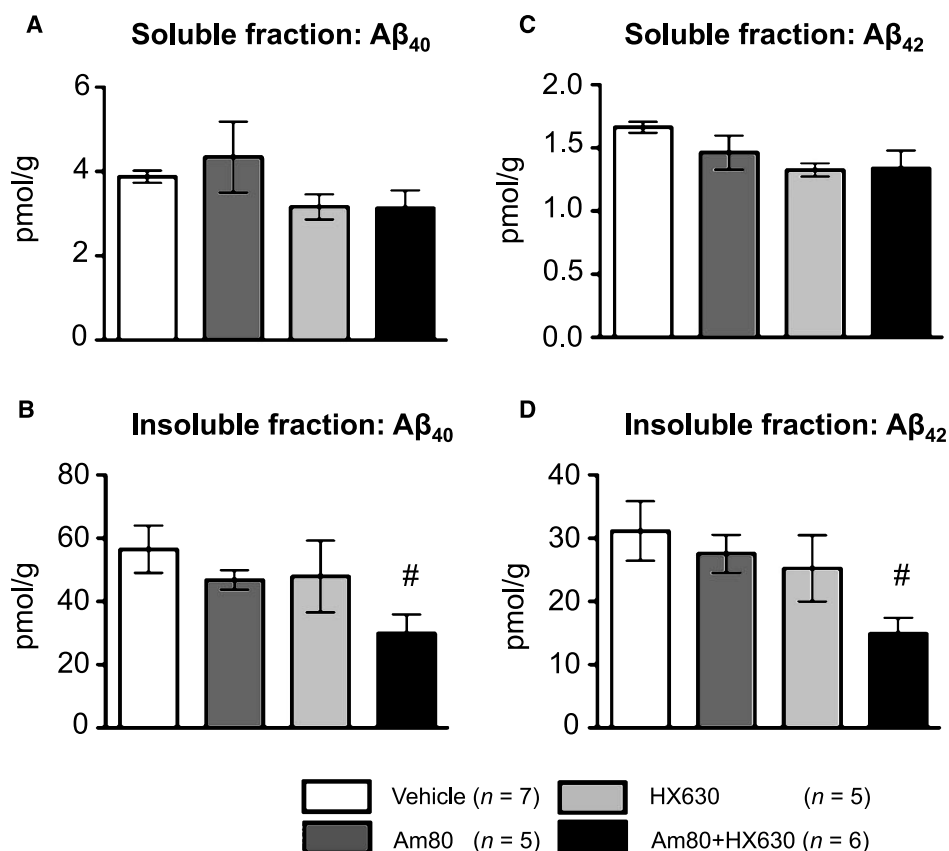
Fig. 2. Co-administration of Am80 (0.5 mg/kg/d) with HX630 (5 mg/kg/d) significantly reduced TBS-insoluble $A\beta_{40}$ and $A\beta_{42}$ levels in the brains of male AβPP23 mice. After the 4-day behavioral study (i.e., at 18 days after the start of treatment), $A\beta_{40}$ (A, B) and $A\beta_{42}$ (C, D) levels in TBS-soluble (A, C) and TBS-insoluble (B, D) fractions of mouse brains were determined by using sandwich ELISA. Error bars represent means ± SEM. #$p < 0.05$ by Dunnett's multiple comparison test, relative to the vehicle-treated groups. No significant difference was observed for the Am80/HX630 group compared to the Am80 and HX630 groups (B, D).

annulus (1.42 ± 0.41) compared with vehicle-treated WT mice (3.90 ± 0.65) (Fig. 1D; $p < 0.01$). After co-administration of Am80 with HX630, however, AβPP23 mice had a significantly higher score (3.22 ± 0.65) than did vehicle-treated AβPP23 mice (Fig. 1D; $p < 0.05$). Thus, co-administration of Am80/HX630 rapidly improved memory deficits in middle-aged AβPP23 mice.

Co-administration of Am80 with HX630 reduced TBS-insoluble $A\beta_{40}$ and $A\beta_{42}$ levels in AβPP23 mouse brains

We used sandwich ELISA to determine and compare the amounts of $A\beta_{40}$ and $A\beta_{42}$ in Tris-buffered saline (TBS)-soluble and -insoluble brain fractions (Fig. 2). Administration of Am80 (0.5 mg/kg/d) or HX630 (5 mg/kg/d) or their combination for 17 days had no effect on levels of $A\beta_{40}$ and $A\beta_{42}$ in the

TBS-soluble brain fraction of 8.5-month-old AβPP23 mice (Fig. 2A, C). In contrast, levels of $A\beta_{40}$ and $A\beta_{42}$ in TBS-insoluble brain fractions were significantly lower in the Am80/HX630-treated group than in the other three groups (Fig. 2B, D). These results indicate that reduction of insoluble Aβ in brain of Am80/HX630-treated mice was correlated with memory improvement. The Aβ levels in 8.5-month-old WT mice were not determined, because preliminary tests showed they were below the detection limit of the ELISA system (data not shown).

Am80/HX630 increased levels of NEP and IDE proteins in vivo

Enzymatic degradation of Aβ peptides and microglia-mediated phagocytosis are involved in Aβ clearance, especially from insoluble fractions [43]. Activated microglia accumulated around amyloid
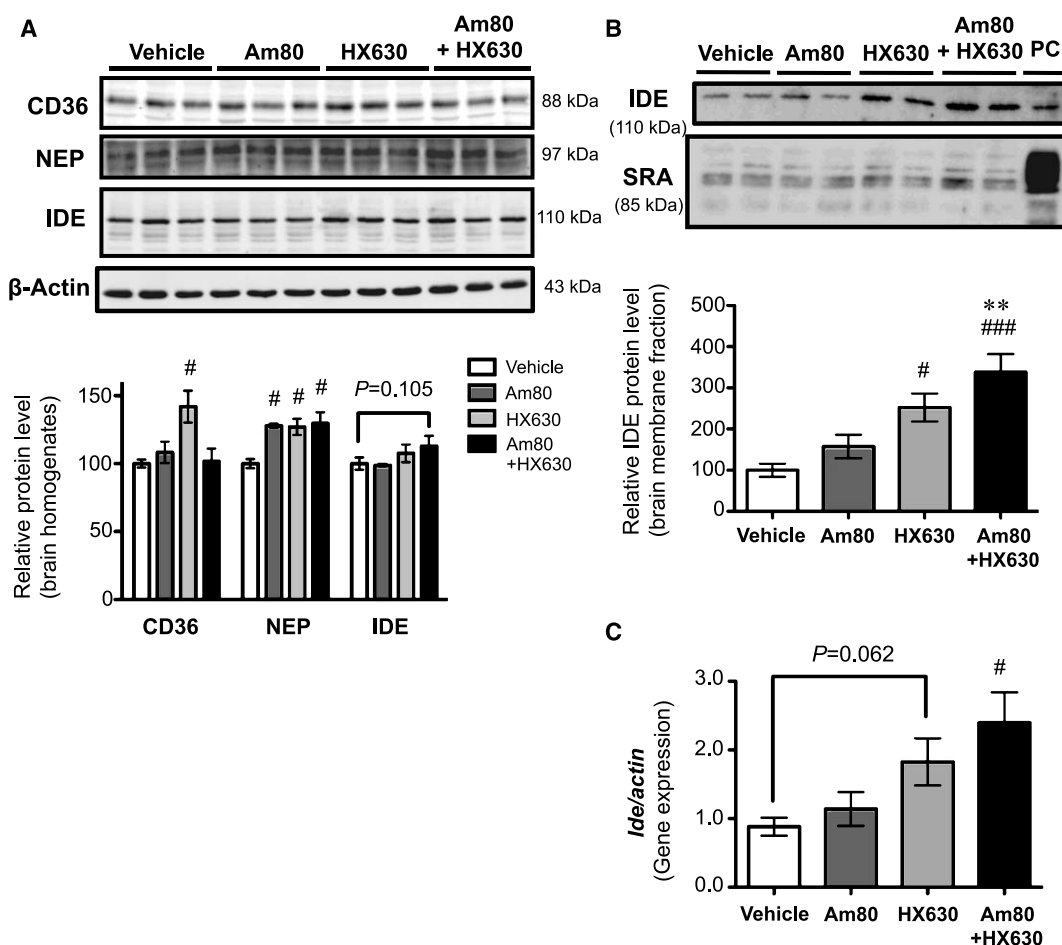
Fig. 3. Am80/HX630 increased NEP and IDE protein levels as well as *Ide* mRNA level in male AβPP23 mice. At 18 days after beginning treatment with Am80 (0.5 mg/kg/d) and/or HX630 (5 mg/kg/d), whole-cell extracts (A), homogenates of the membrane-bound fraction (B), and total RNA were prepared from the brains of AβPP23 mice (A–C). A, B) Immunoblotting with antibodies to CD36, NEP, IDE, β-actin, or SRA was used to study the homogenates (40 μg in A, 5 μg in B). Positive controls (PC) in B are the membrane fractions (5 μg) from brains of WT mice for IDE, and cell lysates from MG5 microglial cells for SRA. The upper panel in B shows representative immunoblotting results of IDE and SRA in the membrane-bound fraction. Densitometric scanning was used to quantify results. Values were normalized to SRA protein expression, and were expressed relative to the vehicle-treated mice. Error bars represent means ± SEM, $n = 3$ (A) and 5 (B) mice per group. $^{###}p < 0.001$ and $^#p < 0.05$ by Dunnett's multiple comparison test, relative to the vehicle-treated group. $^{**}p < 0.01$ by Dunnett's multiple comparison test, relative to the Am80-treated group. C) The RNA samples (1.0 μg) were subjected to quantitative RT-PCR using a specific primer for *Ide* gene. Values were normalized to β-*actin* gene expression. Error bars represent means ± SEM ($n = 3$–4). $^#p < 0.05$ by Dunnett's multiple comparison test, relative to the vehicle-treated AβPP23 mice. $p = 0.062$ by Student's *t*-test for HX630-treated AβPP23 mice, relative to the vehicle-treated AβPP23 mice.

plaques (Supplementary Figure 2A–E) [43] and expressed RARα in vehicle-treated 8.5-month-old male AβPP23 mice (Supplementary Figure 2A–E). Astrocytes also expressed RARα in the vicinity of amyloid plaque (Supplementary Figure 2F–J). It is noteworthy that RARα staining in microglia was almost entirely localized in nuclei, in contrast to the uniformly stained astrocytes, suggesting that RARα was already activated in microglia. Immunoblot analysis of brain samples revealed that the level of scavenger receptor CD36 protein was increased in

HX630-treated mice, but CD36 was not increased after co-administration of HX630 with Am80 (Fig. 3A). Higher levels of NEP protein were found in Am80-, HX630-, and Am80/HX630-treated AβPP23 mice than in vehicle-treated mice (Fig. 3A). The IDE protein level was indistinguishable among the four groups (Fig. 3A). However, the IDE protein level in the membrane-bound fraction was increased significantly in HX630- and Am80/HX630-treated AβPP23 mice compared with vehicle-treated AβPP23 mice (Fig. 3B; $p < 0.05$). The *Ide* mRNA level was also increased
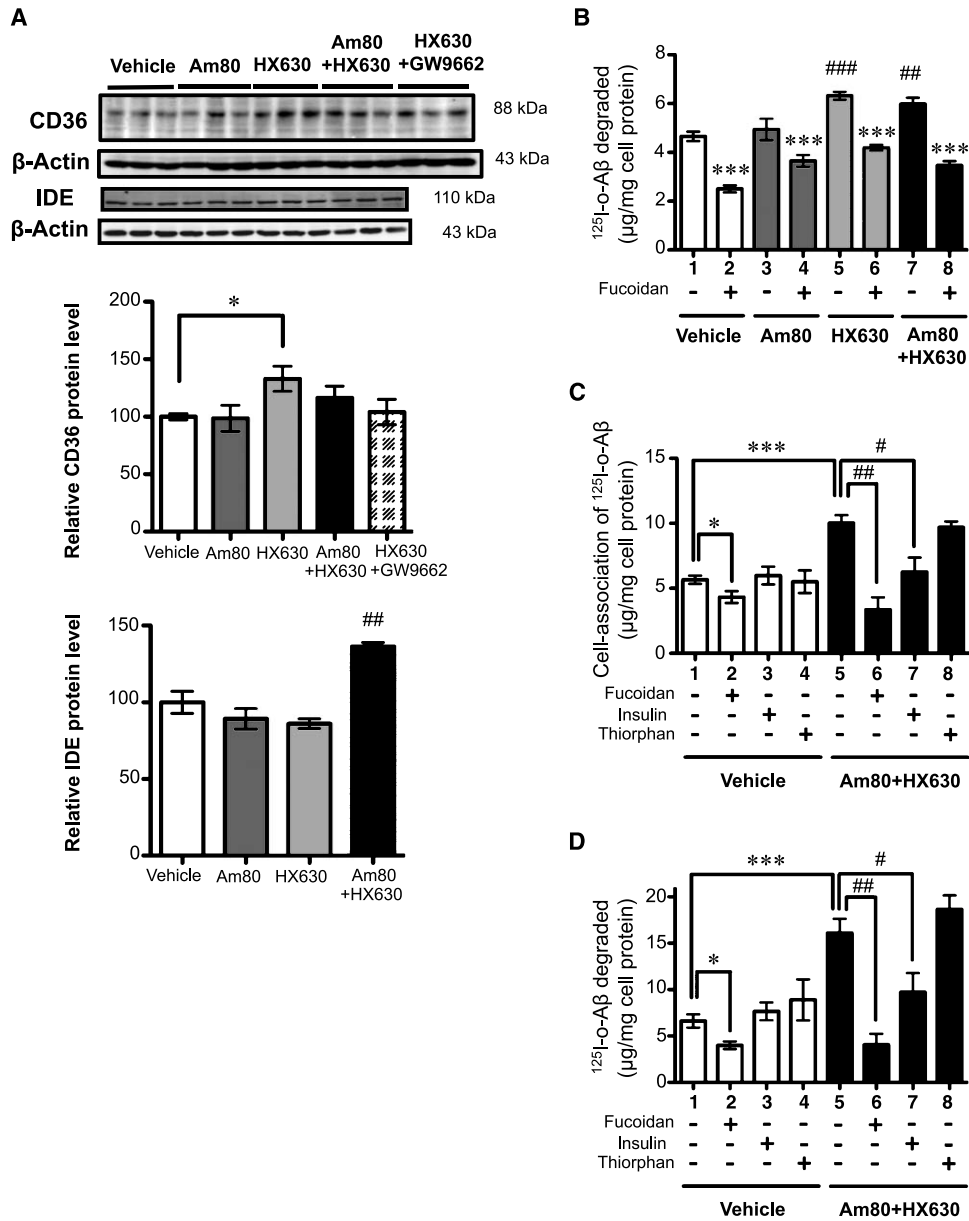
Fig. 4. Clearance of ^{125}I-labeled oligomeric $A\beta_{1-42}$ (o-$A\beta_{1-42}$) by rat primary microglia. A) Rat primary microglia were incubated with Am80 (5 μM) and/or HX630 (5 μM) for 48 h. Cell proteins (30 μg) were subjected to immunoblot analysis with antibodies to CD36, IDE, or β-actin. Densitometric scanning was used to quantify results. Values were normalized to β-actin protein expression, and were expressed relative to those of vehicle-treated cells. Error bars represent means ± SEM ($n = 3$). ##$p < 0.01$ by Dunnett's multiple comparison test, relative to the vehicle-treated cells. B) Cells were cultured for 48 h with Am80 (5 μM) and/or HX630 (5 μM) and then incubated for 6 h with ^{125}I-labeled o-$A\beta_{1-42}$ (1 μg/ml) in the presence or absence of fucoidan (100 μg/ml, a scavenger receptor inhibitor). The amounts of degradation products of ^{125}I-labeled o-Aβ were determined. Error bars represent means ± SEM, $n = 6$. ###$p < 0.001$ and ##$p < 0.01$ by Dunnett's multiple comparison test, relative to the vehicle-treated cells (column 1). ***$p < 0.001$ by Student's t-test, in the presence or absence of fucoidan. C, D) Cells were cultured for 48 h with Am80 (5 μM) and/or HX630 (5 μM) and then incubated for 6 h with ^{125}I-labeled o-$A\beta_{1-42}$ (1 μg/ml) in the presence or absence of fucoidan (100 μg/ml), insulin (100 μg/ml, an IDE inhibitor), or thiorphan (30 μM, a NEP inhibitor). The amounts of cell-association (C) and degradation products (D) of ^{125}I-labeled o-Aβ were determined. Error bars represent means ± SEM, $n = 6$. ***$p < 0.001$ and *$p < 0.05$ by Student's t-test. ##$p < 0.01$ and #$p < 0.05$ for column 5 among columns 5–8, by Dunnett's multiple comparison test.
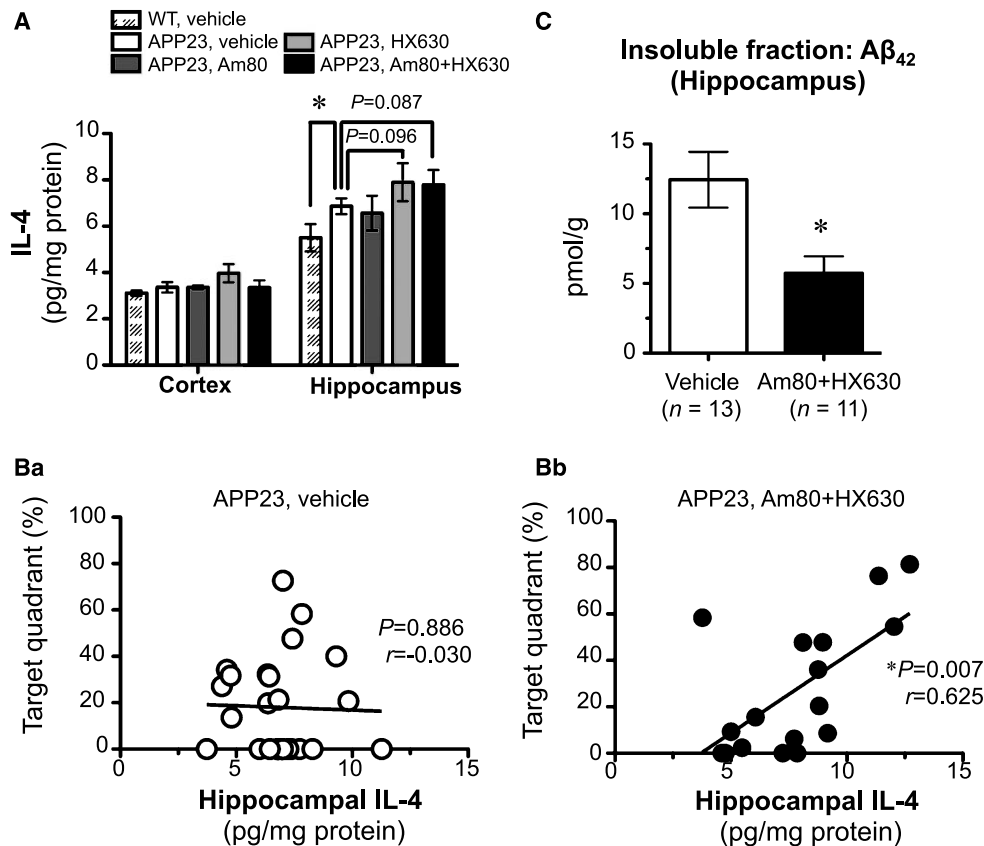
Fig. 5. Am80/HX630-treated male AβPP23 mice showed a significant positive correlation between hippocampal IL-4 levels and performance in the MWM test, but vehicle-treated mice did not. A) At 18 days after beginning treatment with Am80 (0.5 mg/kg/d) and/or HX630 (5 mg/kg/d), levels of IL-4 in TBS-soluble fractions of the cerebral cortex and hippocampus were determined via sandwich ELISA. Error bars represent means ± SEM ($n = 6$ in vehicle-treated WT mice, $n = 25$ in vehicle-treated AβPP23 mice, $n = 5$ in Am80-treated AβPP23 mice, $n = 7$ in HX630-treated AβPP23 mice, $n = 17$ in Am80/HX630-treated AβPP23 mice). B) Scatterplot and Pearson correlation analyses were used to determine the relationship between IL-4 values in the hippocampus and the percent time spent in the target quadrant, for vehicle- (Ba), and Am80/HX630-treated AβPP23 mice (Bb). C) At 18 days after beginning treatment with Am80 (0.5 mg/mg/d) and HX630 (5 mg/kg/d), levels of Aβ42 in TBS-insoluble fractions of the hippocampus were determined via sandwich ELISA. *$p < 0.05$ by Student's t-test.

significantly in Am80/HX630-treated AβPP23 mice compared with the vehicle-treated group (Fig. 3C; $p < 0.05$). The *Ide* mRNA level also showed a slight increase in HX630-treated AβPP23 mice, but this was not statistically significant (Fig. 3C; $p = 0.062$). These results suggest that IDE and NEP may be involved in the increased Aβ clearance in AβPP23 mice treated with Am80/HX630.

Am80/HX630 and HX630 increased clearance activity of oligomeric Aβ peptide in rat primary microglia

We next investigated whether or not Am80 and HX630 increase phagocytotic activity of oligomeric Aβ peptide in microglia *in vitro* (Fig. 4). Recently,

Yamanaka et al. [44] reported that a peroxisome proliferator-activated receptor (PPAR)γ agonist plus an RXR agonist additively upregulated CD36 expression and enhanced microglial uptake of Aβ peptide. CD36 expression was increased 1.3-fold by HX630 treatment, but was not increased in Am80/HX630-treated cells (Fig. 4A). Similar results were also observed *in vivo* (as shown in Fig. 3A). *Cd36* is a target gene of PPARγ/RXR [45]. The increase in CD36 expression by HX630 in microglia was inhibited by co-incubation with the PPARγ antagonist GW9662 (Fig. 4A), indicating that HX630-induced CD36 expression is PPARγ/RXR-dependent. IDE was increased significantly only after co-treatment with Am80/HX630 (Fig. 4A). HX630 and Am80/HX630 increased degradation activity towards ^{125}I-labeled
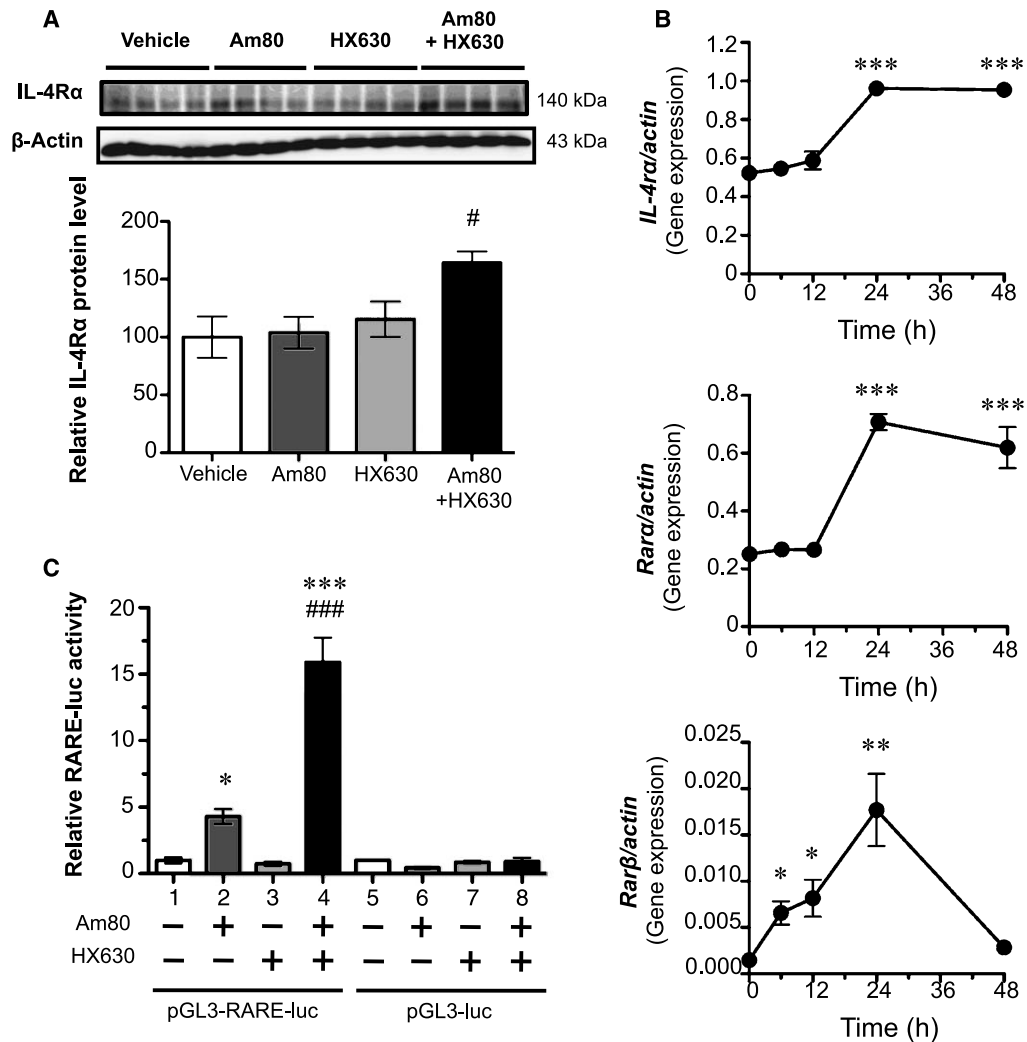
Fig. 6. Am80 with HX630 synergistically increased IL-4Rα protein and RARE reporter activity in mouse microglial MG5 cells. A) MG5 cells were incubated for 48 h with Am80 (5 μM) and/or HX630 (5 μM). Cell proteins (30 μg) were subjected to immunoblot analysis with antibodies to IL-4Rα and β-actin. Densitometric scanning was used to quantify results. Values were normalized to β-actin expression and expressed relative to the vehicle-treated cells. Error bars represent means ± SEM ($n = 4$). $^{\#}p < 0.05$ by Dunnett's multiple comparison test, relative to the vehicle-treated cells. B) RNA from MG5 cells treated with Am80 (5 μM) plus HX630 (5 μM) for indicated periods was subjected to quantitative RT-PCR with specific primers for *Il-4rα, Rarα, Rarβ*, and β-*actin* genes. Total RNA from mouse liver was used as the calibrator sample for *Il-4rα, Rarα, Rarβ*, and β-*actin* genes. Values were normalized to β-*actin* gene expression. Error bars represent means ± SEM ($n = 4$). $^{***}p < 0.001$, $^{**}p < 0.01$, and $^{*}p < 0.05$ by Student's *t*-test, relative to the untreated cells. C) Cells were transfected with the pGL3-RARE-Luc or pGL3-Luc reporter plasmid together with a phRL-TK internal control and were treated with Am80 (5 μM) and/or HX630 (5 μM). Luciferase activity in the cell extract was normalized to *Renilla* luciferase activity and was expressed as fold induction relative to the vehicle-treated cells. Error bars represent means ± SEM ($n = 4$). $^{***}p < 0.001$ and $^{*}p < 0.05$ by Dunnett's multiple comparison test, relative to the vehicle-treated cells (column 1). $^{\#\#\#}p < 0.001$ by Dunnett's multiple comparison test, relative to the Am80-treated cells (column 2).

oligomeric Aβ$_{1-42}$ (o-Aβ$_{1-42}$) in rat primary microglia, compared with vehicle-treated cells, and the increase was inhibited by fucoidan, a scavenger receptor inhibitor, in each case (Fig. 4B). The cell-association and degradation activities in Am80/HX630-treated cells were also inhibited by insulin, an IDE inhibitor

(Fig. 4C, D). The NEP inhibitor thiorphan did not affect the degradation activity in Am80/HX630-treated cells (Fig. 4D). Thus, scavenger receptor-mediated uptake, intracellular degradation and Aβ catabolism by IDE (in cytosol and/or on plasma membrane) are important for Am80/HX630-induced clearance of o-Aβ$_{1-42}$.

Improvement in memory of Am80/HX630-treated AβPP23 mice is correlated with IL-4 levels in the hippocampus

We next investigated whether Am80/HX630-induced memory improvement is related to reduced neuroinflammation, especially changes in levels of anti-inflammatory cytokine IL-4, in the cerebral cortex and hippocampus (Fig. 5). Although the IL-4 level in the cortex was indistinguishable in vehicle-treated WT and AβPP23 mice, the hippocampal IL-4 level was significantly higher in AβPP23 mice than in WT mice (Fig. 5A; $p < 0.05$). HX630 and Am80/HX630 treatments increased the hippocampal IL-4 levels of AβPP23 mice, but the increase was statistically insignificant (Fig. 5A; $p = 0.096$ and $p = 0.087$, respectively). However, the hippocampal IL-4 level in Am80/HX630-treated AβPP23 mice showed a significant positive relationship with memory in the MWM test (Fig. 5Bb; $p = 0.007$, $r = 0.625$). No such correlation was observed for groups treated with vehicle or a single retinoid (Fig. 5Ba, Supplementary Figure 3). The vehicle-treated WT mice also showed a positive correlation between the hippocampal IL-4 level and the MWM memory test performance ($p = 0.072$, $r = 0.772$ for target occupancy, $p = 0.033$, $r = 0.849$ for crossings over the target annulus) (Supplementary Figure 4A, B).

Hippocampal levels of insoluble Aβ$_{42}$ were decreased in Am80/HX630-treated AβPP23 mice (Fig. 5C). These results suggest that memory performance may depend upon the efficiency of IL-4 signaling, not the cytokine levels (Fig. 5A), and that Am80/HX630-induced co-activation of RARα,β/RXRs improves IL-4 signaling.

Am80 and HX630 synergistically increased IL-4Rα expression in mouse microglial MG5 cells

To investigate whether the combination of Am80 and HX630 increases the expression of IL-4 receptor α chain (IL-4Rα) in microglial cells, we examined their effects *in vitro* on mouse microglial MG5 cells (Fig. 6). Am80 and HX630 alone did not increase IL-4Rα levels, but their combination did result in an increase of IL-4Rα (Fig. 6A). IL-4Rα mRNA in MG5 cells was also increased 24–48 hours after Am80/HX630 co-treatment (Fig. 6B). RA response element (RARE) reporter activity in MG5 cells was increased 4.3-fold after Am80 treatment (Fig. 6C), but no increase was seen after HX630 treatment. However, this activity showed a marked increase (15.9-fold)

after co-treatment with HX630 and Am80 (Fig. 6C). In contrast, Am80/HX630 had no effect on the luciferase activity of the control pGL3-luc vector, as expected (Fig. 6C). These results indicate that HX630 has an RAR-synergistic effect in MG5 cells and that marked RAR activity induced by Am80/HX630 may be involved in IL-4Rα upregulation in MG5 cells.

DISCUSSION

Our present results demonstrate that oral co-administration of HX630 (5 mg/kg) and Am80 (0.5 mg/kg) for 17 days ameliorated learning deficits in 8.5-month-old AβPP23 mice (Fig. 1) and significantly reduced brain levels of insoluble Aβ$_{42}$ and Aβ$_{40}$ (Fig. 2). Administration of Am80 alone at higher dose (3 mg/kg/d or 6 mg/kg/d for 17 days) neither reduced Aβ levels nor improved cognitive deficits in AβPP23 mice (Supplementary Figure 5, data not shown).

In contrast, Ding et al. [14] demonstrated that administration of RARs agonist ATRA alone improved memory function in AβPP/PS1 mice. However, ATRA is shown to isomerize to the 9-*cis* isomer *in vitro* [46], which is a potent RARs/RXRs dual agonist, whereas synthetic retinoid Am80 is not converted to derivatives with RXR affinity [47]. Solomin et al. [48], using an RXR-specific reporter transgene, have provided evidence that ATRA (20 mg/kg) activates RXR *in vivo*. An RXR-selective agonist, bexarotene (100 mg/kg, p.o.), improved behavioral defects in AβPP/PS1 mice [16], but it displays cross-reactivity with RARs at higher concentrations [49]. Shudo et al. [13] previously reported that co-administration of Am80/HX630 efficiently ameliorates memory deficits in scopolamine-treated rats, a model of the main clinical symptom of AD. Therefore, it is reasonable to consider that effective memory improvement by retinoids may require RARs/RXRs co-activation. Participation of RARγ is not required for this retinoid-induced improvement in memory deficits, because Am80 is specific for RARα and RARβ and hardly binds to RARγ [50]. Consideration of retinoid receptor selectivity is therefore important for the therapeutic use of retinoids.

Co-administration of Am80 with HX630 reduced the brain level of insoluble, but not soluble, Aβ in AβPP23 mice (Fig. 2). Soluble (TBS-extractable) Aβ is localized mainly in neurons, whereas insoluble Aβ accumulates in extracellular plaques that are formed via oligomers or protofibrils [41, 51]. It is thought that both intracellular and extracellular Aβ oligomers contribute to the pathology of AD

[52]. Tomiyama and colleagues [52] showed that intraneuronal Aβ oligomers are fractionated predominantly into TBS-insoluble fractions, particularly the formic acid-extracted fraction, in AβPP transgenic mice expressing the E693Δ mutation, and contribute to AD via enhanced Aβ oligomerization without fibrillization. Our results here indicate that the apparent reduction of insoluble Aβ correlates well with memory improvement in AβPP23 mice. Mechanisms that may lead to reduced insoluble Aβs consisting intracellular/extracellular Aβ oligomers and extracellular Aβ plaques include the following: (1) increased expression of Aβ-degrading enzymes such as NEP and IDE in neurons and glial cells, and (2) increased internalization or clearance of oligomeric Aβs mainly in microglia. We demonstrated here that these two mechanisms are both functional in retinoid ligand-treated AβPP23 mice.

With regard to the first mechanism, we found that Am80/HX630 treatment increased the expression of the Aβ-degrading enzymes IDE and NEP *in vivo* (Fig. 3). We also observed that Am80/HX630 treatment increased both NEP and IDE in murine N1E115 neuronal cells, and increased NEP in murine A1 glial cells (Supplementary Figure 6). IDE transcription is regulated by RA; the *Ide* gene contains a RARE in its promoter region [53]. We found that Am80/HX630 significantly increased *Ide* mRNA in AβPP23 mice (Fig. 3C). In addition, HX630 tended to increase *Ide* mRNA in AβPP23 mice (Fig. 3C; $p = 0.062$). It is of note that membrane-associated IDE was increased in Am80/HX630- and HX630-treated AβPP23 mice, in parallel with the increase of *Ide* mRNA (Fig. 3B, C), although the IDE level in whole brain lysates was unchanged (Fig. 3A). It has been reported that there are two pools of IDE: a cytosolic pool with a longer half-life and a plasma membrane pool that shows faster turn-over [54]. The membrane-bound IDE protein level is important because its level is related to the clearance of Aβ plaques in AβPP transgenic mice [55] and its decrease in the brain of individuals is associated with a high risk of developing AD [56]. Therefore, the increase in membrane-associated IDE that we observed is considered to contribute to Aβ clearance in Am80/HX630-treated AβPP23 mice. Qui et al. [57] showed that BV2 microglial cells secrete IDE, which mediates the degradation of Aβ peptides in the extracellular milieu. In addition, Goncalves and co-workers [17] showed that IDE activity in the medium was increased in murine microglial cells treated with Am580, an isomer of Am80. Therefore, there is a possibility that IDE is released extracellularly after Am80/HX630 treatment, although the activity in the medium could not be determined in our cell assay system.

NEP, another Aβ-degrading enzyme, was also increased after treatment with Am80, HX630, and their combination in AβPP23 mice (Fig. 3A). The *Mme/Nep* mRNA level, however, was unaffected by these retinoids *in vivo* and *in vitro* (Supplementary Figure 7, data not shown), which suggests that retinoids increase either the translation of *Mme/Nep* mRNA or the stability of the NEP protein. RA reportedly increased RARα-mediated translation of glutamate receptor 1 mRNA in hippocampal neurons [58, 59], and RARα was present in nuclei and dendrites of hippocampal CA1 pyramidal neurons [59], where NEP immunoreactivity was detected in AβPP23 mice [60]. Our results suggest that increased expression of NEP may also contribute to reduction of insoluble Aβ in brain, although NEP expression is not specifically increased by co-administration of Am80/HX630.

It remains unknown whether neprilysin is a target gene of RAR or RXR. It has been reported that neprilysin is a target gene of PPARδ/RXR [61]. It is possible that upregulation of neprilysin by HX630 treatment may depend on PPARδ/RXR activation. In this study, we showed that Am80 as well as Am80/HX630 increased the expression of neprilysin in AβPP23 mice. Further studies are required to elucidate whether neprilysin is a direct target gene of RAR/RXR.

Apropos the second mechanism, we found that HX630 and Am80/HX630 increased phagocytotic activity for oligomeric Aβ peptide in microglia *in vitro* (Fig. 4B). Therefore, increased microglial degradation and clearance of Aβs contribute to the reduction of insoluble Aβ in AβPP23 mice after HX630 and Am80/HX630 treatments. Recently, Yamanaka et al. [44] reported that a PPARγ agonist plus an RXR agonist additively upregulated CD36 expression and enhanced microglial uptake of Aβ peptides. HX630 treatment increased CD36 protein level in microglia (Fig. 4A), suggesting that CD36 may be involved in Aβ clearance in HX630-treated microglia. However, the HX630-induced increase of CD36 expression was abolished by co-treatment with Am80 *in vitro* (Fig. 4A) and *in vivo* (Fig. 3A). In addition, the *Cd36* mRNA level was decreased in Am80/HX630-treated AβPP23 mice (Supplementary Figure 7). We also observed that co-addition of GW9662, a PPARγ antagonist, with HX630 disturbed the HX630-induced CD36 upregulation in microglia (Fig. 4A). Based on these results, we initially speculated that Am80 might block RXR/PPARγ activation by HX630. However, Am80 has been suggested [62] to inhibit *Cd36* tran-

scription in macrophages via mechanisms that are independent of PPARγ, because Am80 does not affect the reporter activity of PPARγ response element. The possibility remains that the Am80-RARα/β complex may outcompete PPARγ for RXR. Thus, the precise mechanism(s) of Am80 inhibition of HX630-induced CD36 expression remains to be solved. We also demonstrated that IDE expression was increased in Am80/HX630-treated microglia, where CD36 expression was decreased (Fig. 4A). The increase of Aβ clearance activity was inhibited by insulin and fucoidan (Fig. 4C). These results indicate that IDE contributes to the Am80/HX630-induced increase of Aβ clearance by enhancing Aβ degradation in microglia.

Thus, we have shown that several factors—Aβ degradation or Aβ clearance systems involving IDE and NEP —are implicated in the reduction of insoluble Aβ and the improvement in memory that we observed in Am80/HX630-treated AβPP23 mice. All these factors together may be responsible for these effects, though we cannot yet assign a priority order for their contributions.

Regarding the participation of inflammation-related cytokines, the hippocampal IL-4 levels and MWM memory test performance showed a significant positive correlation in Am80/HX630-treated AβPP23 mice (Fig. 5Bb), whereas no such correlation was found in the vehicle-treated AβPP23 mice group. The vehicle-treated AβPP23 mice also had higher levels of hippocampal IL-4 than did vehicle-treated WT mice with normal memory function (Fig. 5A), suggesting that functional IL-4 signaling may be impaired in hippocampus of 8.5-month-old AβPP23 mice, and that the AβPP23 mice produce more IL-4 to compensate for the functional defect. We previously showed that intracerebral microinjection of IL-4/IL-13 reduced Aβ levels and improved cognitive deficits in AβPP23 mice, possibly by activating IL-4Rα-positive M2-like microglia [63]. Th2-biased immune responses induced by retinoids may serve to restore IL-4 signaling [23]. A candidate target gene that is impaired in AβPP23 mice is IL-4Rα, as has been reported for aged mice [64]. Immunohistochemical staining showed that IL-4Rα was expressed in the hippocampus (Supplementary Figure 8A), as previously reported [65]. Moreover, the IL-4Rα protein level in the membrane fraction of whole brain, including hippocampus, was increased in Am80/HX630-treated AβPP23 mice compared to the vehicle-treated group (Supplementary Figure 8B). We found here that Am80/HX630 increased IL-4Rα expression in microglial MG5 cells (Fig. 6A,B). Also, HX630 synergistically potentiated

Am80-induced RAR activation in MG5 cells (Fig. 6C). Therefore, Am80/HX630 may promote differentiation of IL-4-responsive M2-like microglia and increase their clearance activity for oligomeric Aβ peptides by restoring impaired IL-4 signaling in AβPP23 mice. The present results are consistent with reports that alternative microglial activation via IL-4 signaling is impaired in AD [3].

We have not determined whether IL-4Rα is a target gene of either RAR or RXR. However, Zhu and colleagues [66] showed that ATRA markedly increased mRNAs encoding RARβ and IL-4Rα in murine dendritic cells, and RARβ bound directly with the promoter region of IL-4Rα following ATRA treatment [66]. As shown in Fig. 6B, Rarβ mRNA was increased 6 h after Am80/HX630 treatment and reached a maximum at 24 h in murine MG5 microglial cells. On the other hand, IL-4Rα mRNA was expressed before treatment, then began to increase at 24 h after treatment, and remained little changed up to 48 h. These results suggest that the IL-4Rα induction is mediated by RARβ in Am80/HX630-treated cells. The Rarα gene contains RARE motifs in its promoter region [67, 68], and Rarα mRNA was also increased at 24–48 h after Am80/HX630 treatment (Fig. 6B). In Am80-treated MG5 cells, RARE-reporter activity was increased, but IL-4Rα protein expression remained unchanged (Fig. 6A, 6C). IDE protein, another target gene of RAR/RXR was increased by Am80/HX630, but not by Am80 in MG5 cells and rat microglia (Fig. 4A, Supplementary Figure 9). These results suggest that co-activation of RAR/RXR might be required for efficient protein expression of RAR/RXR target genes in microglia.

Proinflammatory cytokines have been implicated in sickness-associated behaviors, aging, and autoimmunity [25], whereas cytokines associated with classical inflammation are required for many aspects of CNS function, such as synaptic scaling through glial TNF-α [69]. We observed that hippocampal TNF-α levels also showed a positive correlation with memory test performance in Am80/HX630-treated AβPP23 mice (Supplementary Figures 10Bd, 11Cd), but not in the vehicle-treated group (Supplementary Figures 10Ba, 11Ca). Levels of hippocampal mRNAs for Tnfr1 and 2 in AβPP23 mice were higher than those in WT mice (Supplementary Figure 12A,B). Therefore, we believe that TNF-α signaling, not TNF-α amount (Supplementary Figure 10A), may be impaired in AβPP23 mice. The present result is also consistent with reports that homeostatic synaptic scaling via TNF-α signaling is impaired in AD [70, 71].

In the present study, the hippocampal TNF-α level in Am80-treated AβPP23 mice showed a positive relationship with memory in the MWM test ($p = 0.084$, $r = 0.827$ for target occupancy, $p = 0.055$, $r = 0.870$ for crossings over the target annulus) (Supplementary Figures 10Bb, 11Cb). However, Am80 treatment did not ameliorate memory deficits in AβPP23 mice (Fig. 1), which suggests that improved hippocampal TNF-α signaling is important but not sufficient for memory improvement in 8.5-month-old AβPP23 mice. Consequently, co-activation of RAR and RXR by co-administration of Am80 with HX630 may ameliorate memory deficits in AβPP23 mice by improving both TNF-α and IL-4 signaling. However, further study is needed to confirm this idea.

The present *in vivo* data are not consistent with the *in vitro* study of Dheen et al. [72], who reported that Aβ peptide activates TNF-α expression, and also that this activation is reduced by ATRA treatment. However, the inhibitory effect of ATRA on TNF-α production was only moderate (about 40–50%), in contrast to its complete inhibition of nitric oxide production [72, 73]. In an AD model mouse, loss of both TNFR1 and TNFR2 exacerbates the pathogenesis and reduces Aβ phagocytic activity in microglia, indicating that intact TNF-α receptor signaling is critical for microglial-mediated uptake of the extracellular Aβ peptide pool [71]. Overall, these reports suggest that TNF-α produced by activated microglial cells is pleiotropic and may be either neuroprotective or neurotoxic depending on several factors, for example, which type of TNF receptor is activated [71, 74].

In this study, we observed that RARα is located in nuclei of microglia, but is dispersed throughout astrocytes in AβPP23 mice (Supplementary Figure 2). Thus, when microglia accumulate around Aβ plaques in AβPP23 mice, their RARα appears to be activated, and Aβ clearance is increased. However, the ability of microglia to clear Aβ is considered to decrease with age and progression of AD pathology [75]. Goncalves et al. [17] recently showed that RARα signaling is down-regulated by Aβ, which inhibits the synthesis of the endogenous ligand, RA, in AβPP mice (Tg2576). Although we observed nuclear translocation of RARα in microglia of AβPP23 mice, this may be insufficient to enable transcriptional activation by endogenous RA in the mice, and exogenous Am80 may be required to achieve activation. We did not examine whether transcriptional activation of RARα is decreased in AβPP23 mice compared to their WT littermates. However, we observed that the expression level of mRNA for tissue-plasminogen activator (tPA),

one of the genes controlled by RAR/RXR, tended to be lower than that in WT littermates ($p = 0.080$, Supplementary Figure 13B), whereas it was significantly increased in Am80/HX630-treated AβPP23 mice compared to vehicle-treated AβPP23 mice (Supplementary Figure 13B). Moreover, *Ide* is a target gene of RAR/RXR, and *Ide* mRNA was decreased in microglia of AβPP/PS1 mice at the age of 8 months, compared to that in microglia of their WT littermates [75]. Further study is needed to investigate whether the expression levels of RARα-target genes in microglia are decreased in AβPP23 mice and whether they are increased by Am80/HX630 administration *in vivo*.

It is not clear whether Am80 and HX630 cross the blood-brain barrier and directly or indirectly affect the brain. It is known that Am580, an isomer of Am80, crosses the blood-brain barrier in mice [17]. Am80 has been reported to attain some extent of access into the brain: cerebral tissue content of Am80 in normal male rats reaches around 100 pmol/g tissue at 2 h after subcutaneous administration of the drug at 1 mg/kg, then decreased at 6 h, and returned to the control levels at 24–120 h [76, 77]. *Rarβ* is a target gene of RAR/RXR, and *Rarβ* mRNA was not increased by Am80/HX630 treatment *in vivo* (Supplementary Figure 13A), in contrast to the *in vitro* study (Fig. 6). Because brain tissues were sampled at 1 day after last administration of the compounds, the concentration is considered not to be enough to increase *Rarβ* mRNA expression at the time point. The expression level of *Rarβ* mRNA may be tightly regulated (probably by a transcription factor), or the half-life of *Rarβ* mRNA may be short *in vivo*. On the other hand, the expression of *Ide*, another RAR/RXR-target gene, was increased by Am80/HX630 treatment *in vivo* as well as *in vitro* (Figs. 3C, 4A). Moreover, mRNA for *tPA*, another target gene of RAR/RXR, was also increased by Am80/HX630 co-administration (Supplementary Figure 13B). mRNA and protein of *Cd36*, a target gene of PPARγ/RXR, were increased by HX630 treatment both *in vitro* and *in vivo* (Figs. 3A, 4A). These results suggest that Am80 and HX630 might cross the blood-brain barrier and act directly in the brain.

Finally, we should mention that Goncalves et al. [17] recently reported that Am580 (an Am80 isomer with a reversed amide bond) ameliorated cognitive deficits (T-maze spontaneous alternation and Nest building tests) in Tg2576 mice, another AD model. Although the method of administration, kinds of behavioral experiments, and AD model were different from ours, we speculate that combined treatment with Am580 and an

RXR ligand might also be synergistically more effective on memory deficits (MWM) in their model.

In conclusion, co-administration of Am80/HX630 effectively reduces insoluble Aβ peptides and improves cognitive deficits in AβPP23 mice. Combination treatment with RAR and RXR agonists, therefore, may be an effective approach for AD therapy.

ACKNOWLEDGMENTS

Authors' disclosures available online (http://www.j-alz.com/disclosures/view.php?id=2274).

SUPPLEMENTARY MATERIAL

Supplementary figures are available in the electronic version of this article: http://dx.doi.org/10.3233/JAD-132720.

REFERENCES

[1]   Krstic D, Knuesel I (2013) Deciphering the mechanism underlying late-onset Alzheimer's disease. *Nat Rev Neurol* **9**, 25-34.

[2]   Vom Berg J, Prokop S, Miller KR, Obst J, Kälin RE, Lopategui-Cabezas I, Wegner A, Mair F, Schipke CG, Peters O, Winter Y, Becher B, Heppner FL (2012) Inhibition of IL-12/IL-23 signaling reduces Alzheimer's disease-like pathology and cognitive decline. *Nat Med* **18**, 1812-1819.

[3]   Heneka MT, Kummer MP, Stutz A, Delekate A, Schwartz S, Vieira-Saecker A, Griep A, Axt D, Remus A, Tzeng TC, Gelpi E, Halle A, Korte M, Latz E, Golenbock DT (2013) NLRP3 is activated in Alzheimer's disease and contributes to pathology in APP/PS1 mice. *Nature* **493**, 674-678.

[4]   Sporn MB, Roberts AB, Goodman DS, Gudas LJ (1994) *The Retinoids: Biology, Chemistry, and Medicine, 2nd ed*, Raven Press, New York.

[5]   Corcoran JP, So PL, Maden M (2004) Disruption of the retinoid signalling pathway causes a deposition of amyloid β in the adult rat brain. *Eur J Neurosci* **20**, 896-902.

[6]   Prinzen C, Müller U, Endres K, Fahrenholz F, Postina R (2005) Genomic structure and functional characterization of the human ADAM10 promoter. *FASEB J* **19**, 1522-1524.

[7]   Tippmann F, Hundt J, Schneider A, Endres K, Fahrenholz F (2009) Up-regulation of the α-secretase ADAM10 by retinoic acid receptors and acitretin. *FASEB J* **23**, 1643-1654.

[8]   Jarvis CI, Goncalves MB, Clarke E, Dogruel M, Kalindjian SB, Thomas SA, Maden M, Corcoran JP (2010) Retinoic acid receptor-α signalling antagonizes both intracellular and extracellular amyloid-β production and prevents neuronal cell death caused by amyloid-β. *Eur J Neurosci* **32**, 1246-1255.

[9]   Koryakina A, Aeberhard J, Kiefer S, Hamburger M, Küenzi P (2009) Regulation of secretases by all-trans-retinoic acid. *FEBS J* **276**, 2645-2655.

[10]   Lichtenthaler SF (2011) α-Secretase in Alzheimer's disease: Molecular identity, regulation and therapeutic potential. *J Neurochem* **116**, 10-21.

[11]   Endres K, Fahrenholz F (2012) Regulation of α-secretase ADAM10 expression and activity. *Exp Brain Res* **217**, 343-352.

[12]   Goodman AB, Pardee AB (2003) Evidence for defective retinoid transport and function in late onset Alzheimer's disease. *Proc Natl Acad Sci U S A* **100**, 2901-2905.

[13]   Shudo K, Kagechika H, Yamazaki N, Igarashi M, Takeda C (2004) A synthetic retinoid Am80 (tamibarotene) rescues the memory deficit caused by scopolamine in a passive avoidance paradigm. *Biol Pharm Bull* **27**, 1887-1889.

[14]   Ding Y, Qiao A, Wang Z, Goodwin JS, Lee ES, Block ML, Allsbrook M, McDonald MP, Fan GH (2008) Retinoic acid attenuates β-amyloid deposition and rescues memory deficits in an Alzheimer's disease transgenic mouse model. *J Neurosci* **28**, 11622-11634.

[15]   Kawahara K, Nishi K, Suenobu M, Ohtsuka H, Maeda A, Nagatomo K, Kuniyasu A, Staufenbiel M, Nakagomi M, Shudo K, Nakayama H (2009) Oral administration of synthetic retinoid Am80 (Tamibarotene) decreases brain β-amyloid peptides in APP23 mice. *Biol Pharm Bull* **32**, 1307-1309.

[16]   Cramer PE, Cirrito JR, Wesson DW, Lee CY, Karlo JC, Zinn AE, Casali BT, Restivo JL, Goebel WD, James MJ, Brunden KR, Wilson DA, Landreth GE (2012) ApoE-directed therapeutics rapidly clear β-amyloid and reverse deficits in AD mouse models. *Science* **335**, 1503-1506.

[17]   Goncalves MB, Clarke E, Hobbs C, Malmqvist T, Deacon R, Jack J, Corcoran JP (2013) Amyloid β inhibits retinoic acid synthesis exacerbating Alzheimer disease pathology which can be attenuated by an retinoic acid receptor α agonist. *Eur J Neurosci* **37**, 1182-1192.

[18]   Fitz NF, Cronican AA, Lefterov I, Koldamova R (2013) Comment on "ApoE-directed therapeutics rapidly clear β-amyloid and reverse deficits in AD mouse models". *Science* **340**, 924-c.

[19]   Price AR, Xu G, Siemienski ZB, Smithson LA, Borchelt DR, Golde TE, Felsenstein KM (2013) Comment on "ApoE-directed therapeutics rapidly clear β-amyloid and reverse deficits in AD mouse models". *Science* **340**, 924-d.

[20]   Tesseur I, Lo AC, Roberfroid A, Dietvorst S, Van Broeck B, Borgers M, Gijsen H, Moechars D, Mercken M, Kemp J, D'Hooge R, De Strooper B (2013) Comment on "ApoE-directed therapeutics rapidly clear β-amyloid and reverse deficits in AD mouse models". *Science* **340**, 924-e.

[21]   Veeraraghavalu K, Zhang C, Miller S, Hefendehl JK, Rajapaksha TW, Ulrich J, Jucker M, Holtzman DM, Tanzi RE, Vassar R, Sisodia SS (2013) Comment on "ApoE-directed therapeutics rapidly clear β-amyloid and reverse deficits in AD mouse models". *Science* **340**, 924-f.

[22]   LaClair KD, Manaye KF, Lee DL, Allard JS, Savonenko AV, Troncoso JC, Wong PC (2013) Treatment with bexarotene, a compound that increases apolipoprotein-E, provides no cognitive benefit in mutant APP/PS1 mice. *Mol Neurodegener* **8**, 18.

[23]   Ross AC (2012) Vitamin A and retinoic acid in T cell-related immunity. *Am J Clin Nutr* **96**, 1166S-1172S.

[24]   Iwata M, Eshima Y, Kagechika H (2003) Retinoic acids exert direct effects on T cells to suppress Th1 development and enhance Th2 development via retinoic acid receptors. *Int Immunol* **15**, 1017-1025.

[25] Gadani SP, Cronk JC, Norris GT, Kipnis J (2012) IL-4 in the brain: A cytokine to remember. *J Immunol* **189**, 4213-4219.

[26] Derecki NC, Cardani AN, Yang CH, Quinnies KM, Crihfield A, Lynch KR, Kipnis J (2010) Regulation of learning and memory by meningeal immunity: A key role for IL-4. *J Exp Med* **207**, 1067-1080.

[27] Delescluse C, Cavey MT, Martin B, Bernard BA, Reichert U, Maignan J, Darmon M, Shroot B (1991) Selective high affinity retinoic acid receptor alpha or beta-gamma ligands. *Mol Pharmacol* **40**, 556-562.

[28] Amano Y, Noguchi M, Nakagomi M, Muratake H, Fukasawa H, Shudo K (2013) Design, synthesis and evaluation of retinoids with novel bulky hydrophobic partial structures. *Bioorg Med Chem* **21**, 4342-4350.

[29] Ishida S, Shigemoto-Mogami Y, Kagechika H, Shudo K, Ozawa S, Sawada J, Ohno Y, Inoue K (2003) Clinically potential subclasses of retinoid synergists revealed by gene expression profiling. *Mol Cancer Ther* **2**, 49-58.

[30] Nishimaki-Mogami T, Tamehiro N, Sato Y, Okuhira K, Sai K, Kagechika H, Shudo K, Abe-Dohmae S, Yokoyama S, Ohno Y, Inoue K, Sawada J (2008) The RXR agonists PA024 and HX630 have different abilities to activate LXR/RXR and to induce ABCA1 expression in macrophage cell lines. *Biochem Pharmacol* **76**, 1006-1013.

[31] Kagechika H, Kawachi E, Hashimoto Y, Shudo K (1984) New type inducers of differentiation of human HL-60 promyelocytic leukemia cells. Terephthalic anilides. *Chem Pharm Bull* **32**, 4209-4212.

[32] Umemiya H, Fukasawa H, Ebisawa M, Eyrolles L, Kawachi E, Eisenmann G, Gronemeyer H, Hashimoto Y, Shudo K, Kagechika H (1997) Regulation of retinoidal actions by diazepinylbenzoic acids. Retinoid synergists which activate the RXR-RAR heterodimers. *J Med Chem* **40**, 4222-4234.

[33] Sturchler-Pierrat C, Abramowski D, Duke M, Wiederhold KH, Mistl C, Rothacher S, Ledermann B, Bürki K, Frey P, Paganetti PA, Waridel C, Calhoun ME, Jucker M, Probst A, Staufenbiel M, Sommer B (1997) Two amyloid precursor protein transgenic mouse models with Alzheimer disease-like pathology. *Proc Natl Acad Sci U S A* **94**, 13287-13292.

[34] Shimizu E, Kawahara K, Kajizono M, Sawada M, Nakayama H (2008) IL-4-induced selective clearance of oligomeric β-amyloid peptide1-42 by rat primary type 2 microglia. *J Immunol* **181**, 6503-6513.

[35] Ohsawa K, Imai Y, Nakajima K, Kohsaka S (1997) Generation and characterization of a microglial cell line, MG5, derived from a p53-deficient mouse. *Glia* **21**, 285-298.

[36] Dam DV, D'Hooge R, Staufenbiel M, Ginneken CV, Meir FV, De Deyn PP (2003) Age-dependent cognitive decline in the APP23 model precedes amyloid deposition. *Eur J Neurosci* **17**, 388-396.

[37] Ishido M, Shudo K (2009) Oral administration of synthetic retinoid Am80 inhibits the development of type 1 diabetes in non-obese diabetic (NOD) mice. *Biol Pharm Bull* **32**, 157-159.

[38] Morris R (1984) Developments of a water-maze procedure for studying spatial learning in the rat. *J Neurosci Methods* **11**, 47-60.

[39] Vorhees CV, Williams MT (2006) Morris water maze: Procedures for assessing spatial and related forms of learning and memory. *Nat Protoc* **1**, 848-858.

[40] Iwata N, Takaki Y, Fukami S, Tsubuki S, Saido TC (2002) Region-specific reduction of Aβ-degrading endopeptidase, neprilysin, in mouse hippocampus upon aging. *J Neurosci Res* **70**, 493-500.

[41] Huang SM, Mouri A, Kokubo H, Nakajima R, Suemoto T, Higuchi M, Staufenbiel M, Noda Y, Yamaguchi H, Nabeshima T, Saido TC, Iwata N (2006) Neprilysin-sensitive synapse-associated amyloid-β peptide oligomers impair neuronal plasticity and cognitive function. *J Biol Chem* **281**, 17941-17951.

[42] Chomczynski P, Sacchi N (1987) Single-step method of RNA isolation by acid guanidinium thiocyanate-phenol-chloroform extraction. *Anal Biochem* **162**, 156-159.

[43] Mildner A, Schlevogt B, Kierdorf K, Böttcher C, Erny D, Kummer MP, Quinn M, Brück W, Bechmann I, Heneka MT, Priller J, Prinz M (2011) Distinct and non-redundant roles of microglia and myeloid subsets in mouse models of Alzheimer's disease. *J Neurosci* **31**, 11159-11171.

[44] Yamanaka M, Ishikawa T, Griep A, Axt D, Kummer MP, Heneka MT (2012) PPARγ/RXRα-induced and CD36-mediated microglial amyloid-β phagocytosis results in cognitive improvement in amyloid precursor protein/presenilin 1 mice. *J Neurosci* **32**, 17321-17331.

[45] Tontonoz P, Nagy L, Alvarez JG, Thomazy VA, Evans RM (1998) PPARγ promotes monocyte/macrophage differentiation and uptake of oxidized LDL. *Cell* **93**, 241-252.

[46] Heyman RA, Mangelsdorf DJ, Dyck JA, Stein RB, Eichele G, Evans RM, Thaller C (1992) 9-cis Retinoic acid is a high affinity ligand for the retinoid X receptor. *Cell* **68**, 397-406.

[47] Miwako I, Kagechika H (2007) Tamibarotene. *Drugs Today* **43**, 563-568.

[48] Solomin L, Johansson CB, Zetterström RH, Bissonnette RP, Heyman RA, Olson L, Lendahl U, Frisén J, Perlmann T (1998) Retinoid-X receptor signalling in the developing spinal cord. *Nature* **395**, 398-402.

[49] Zhang C, Hazarika P, Ni X, Weidner DA, Duvic M (2002) Induction of apoptosis by bexarotene in cutaneous T-cell lymphoma cells: Relevance to mechanism of therapeutic action. *Clin Cancer Res* **8**, 1234-1240.

[50] Kagechika H, Shudo K (2005) Synthetic retinoids: Recent developments concerning structure and clinical utility. *J Med Chem* **48**, 5875-5883.

[51] Oddo S, Caccamo A, Smith IF, Green KN, LaFerla FM (2006) A dynamic relationship between intracellular and extracellular pools of Aβ. *Am J Pathol* **168**, 184-194.

[52] Tomiyama T, Matsuyama S, Iso H, Umeda T, Takuma H, Ohnishi K, Ishibashi K, Teraoka R, Sakama N, Yamashita T, Nishitsuji K, Ito K, Shimada H, Lambert MP, Klein WL, Mori H (2010) A mouse model of amyloid β oligomers: Their contribution to synaptic alteration, abnormal tau phosphorylation, glial activation, and neuronal loss *in vivo*. *J Neurosci* **30**, 4845-4856.

[53] Melino G, Draoui M, Bernardini S, Bellincampi L, Reichert U, Cohen P (1996) Regulation by retinoic acid of insulin-degrading enzyme and of a related endoprotease in human neuroblastoma cell lines. *Cell Growth Differ* **7**, 787-796.

[54] Bulloj A, Leal MC, Surace EI, Zhang X, Xu H, Ledesma MD, Castaño EM, Morelli L (2008) Detergent resistant membrane-associated IDE in brain tissue and cultured cells: Relevance to Aβ and insulin degradation. *Mol Neurodegener* **3**, 22.

[55] Killick R, Scales G, Leroy K, Causevic M, Hooper C, Irvine EE, Choudhury AI, Drinkwater L, Kerr F, Al-Qassab H, Stephenson J, Yilmaz Z, Giese KP, Brion JP, Withers DJ, Lovestone S (2009) Deletion of Irs2 reduces amyloid deposition and rescues behavioural deficits in APP transgenic mice. *Biochem Biophys Res Commun* **386**, 257-262.

[56] Zhao Z, Xiang Z, Haroutunian V, Buxbaum JD, Stetka B, Pasinetti GM (2007) Insulin degrading enzyme activity selectively decreases in the hippocampal formation of cases at

high risk to develop Alzheimer's disease. *Neurobiol Aging* **28**, 824-830.

[57] Qiu WQ, Walsh DM, Ye Z, Vekrellis K, Zhang J, Podlisny MB, Rosner MR, Safavi A, Hersh LB, Selkoe DJ (1998) Insulin-degrading enzyme regulates extracellular levels of amyloid β-protein by degradation. *J Biol Chem* **273**, 32730-32738.

[58] Maghsoodi B, Poon MM, Nam CI, Aoto J, Ting P, Chen L (2008) Retinoic acid regulates RARα-mediated control of translation in dendritic RNA granules during homeostatic synaptic plasticity. *Proc Natl Acad Sci U S A* **105**, 16015-16020.

[59] Poon MM, Chen L (2008) Retinoic acid-gated sequence-specific translational control by RARα. *Proc Natl Acad Sci U S A* **105**, 20303-20308.

[60] Higuchi M, Iwata N, Matsuba Y, Takano J, Suemoto T, Maeda J, Ji B, Ono M, Staufenbiel M, Suhara T, Saido TC (2012) Mechanistic involvement of the calpain-calpastatin system in Alzheimer neuropathology. *FASEB J* **26**, 1204-1217.

[61] Kalinin S, Richardson JC, Feinstein DL (2009) A PPARδ agonist reduces amyloid burden and brain inflammation in a transgenic mouse model of Alzheimer's disease. *Curr Alzheimer Res* **6**, 431-437.

[62] Takeda N, Manabe I, Shindo T, Iwata H, Iimuro S, Kagechika H, Shudo K, Nagai R (2006) Synthetic retinoid Am80 reduces scavenger receptor expression and atherosclerosis in mice by inhibiting IL-6. *Arterioscler Thromb Vasc Biol* **26**, 1177-1183.

[63] Kawahara K, Suenobu M, Yoshida A, Koga K, Hyodo A, Ohtsuka H, Kuniyasu A, Tamamaki N, Sugimoto Y, Nakayama H (2012) Intracerebral microinjection of interleukin-4/interleukin-13 reduces β-amyloid accumulation in the ipsilateral side and improves cognitive deficits in young amyloid precursor protein 23 mice. *Neuroscience* **207**, 243-260.

[64] Fenn AM, Henry CJ, Huang Y, Dugan A, Godbout JP (2012) Lipopolysaccharide-induced interleukin (IL)-4 receptor-α expression and corresponding sensitivity to the M2 promoting effects of IL-4 are impaired in microglia of aged mice. *Brain Behav Immun* **26**, 766-777.

[65] Nolan Y, Maher FO, Martin DS, Clarke RM, Brady MT, Bolton AE, Mills KH, Lynch MA (2005) Role of interleukin-4 in regulation of age-related inflammatory changes in the hippocampus. *J Biol Chem* **280**, 9354-9362.

[66] Zhu B, Buttrick T, Bassil R, Zhu C, Olah M, Wu C, Xiao S, Orent W, Elyaman W, Khoury SJ (2013) IL-4 and retinoic acid

synergistically induce regulatory dendritic cells expressing Aldh1a2. *J Immunol* **191**, 3139-3151.

[67] Carpentier A, Balitrand N, Rochette-Egly C, Shroot B, Degos L, Chomienne C (1997) Distinct sensitivity of neuroblastoma cells for retinoid receptor agonists: Evidence for functional receptor heterodimers. *Oncogene* **15**, 1805-1813.

[68] Leroy P, Nakshatri H, Chambon P (1991) Mouse retinoic acid receptor α2 isoform is transcribed from a promoter that contains a retinoic acid response element. *Proc Natl Acad Sci U S A* **88**, 10138-10142.

[69] Stellwagen D, Malenka RC (2006) Synaptic scaling mediated by glial TNF-α. *Nature* **440**, 1054-1059.

[70] Chang EH, Savage MJ, Flood DG, Thomas JM, Levy RB, Mahadomrongkul V, Shirao T, Aoki C, Huerta PT (2006) AMPA receptor downscaling at the onset of Alzheimer's disease pathology in double knockin mice. *Proc Natl Acad Sci U S A* **103**, 3410-3415.

[71] Montgomery SL, Mastrangelo MA, Habib D, Narrow WC, Knowlden SA, Wright TW, Bowers WJ (2011) Ablation of TNF-RI/RII expression in Alzheimer's disease mice leads to an unexpected enhancement of pathology: Implications for chronic pan-TNF-α suppressive therapeutic strategies in the brain. *Am J Pathol* **179**, 2053-2070.

[72] Dheen ST, Jun Y, Yan Z, Tay SS, Ling EA (2005) Retinoic acid inhibits expression of TNF-α and iNOS in activated rat microglia. *Glia* **50**, 21-31.

[73] Hellmann-Regen J, Kronenberg G, Uhlemann R, Freyer D, Endres M, Gertz K (2013) Accelerated degradation of retinoic acid by activated microglia. *J Neuroimmunol* **256**, 1-6.

[74] Santello M, Volterra A (2012) TNFα in synaptic function: Switching gears. *Trends Neurosci* **35**, 638-647.

[75] Hickman SE, Allison EK, El Khoury J (2008) Microglial dysfunction and defective beta-amyloid clearance pathways in aging Alzheimer's disease mice. *J Neurosci* **28**, 8354-8360.

[76] Mizojiri K, Okabe H, Sugeno K, Esumi Y, Takaichi M, Miyake T, Seki H, Inaba A (1997) Studies on the metabolism and disposition of the new retinoid 4-[(5,6,7,8-tetrahydro-5,5,8,8-tetramethyl-2-naphthyl)carbamoyl] benzoic acid. 1st communication: Absorption, distribution, metabolism and excretion after topical application and subcutaneous administration in rats. *Arzneimittelforschung* **47**, 59-69.

[77] Liu X, Zhang Z, Jiang Y, Hu Y, Wang Z, Liu J, Feng R, Zhang J, Huang G (2014) Novel PEG-grafted nanostructured lipid carrier for systematic delivery of a poorly soluble anti-leukemia agent Tamibarotene: Characterization and evaluation. *Drug Deliv*, doi:10.3109/10717544.2014.885614